Core-Shell Particles: Building Blocks for Advanced Polymer Materials

*Hung H. Pham, Eugenia Kumacheva**

Department of Chemistry, University of Toronto, 80 St. George Street, Toronto, Ontario, Canada, M5S 3H6

Summary: Polymer particles with submicrometer dimensions show promising applications in "bottom-to-top approach" to fabrication of materials with periodic structure, function, and composition. A novel approach to producing such materials is proposed, which employs core-shell particles with specific structures and compositions. We report on the synthesis of core-shell particles using interfacial polymerization and heterocoagulation techniques. The compositions of core-forming material and/or the shell-forming polymers were selectively controlled to be make the cores or the shells rigid or fluid, fluorescent or non-fluorescent, organic or inorganic. Several potential applications of nanocomposite materials obtained from these particles are demonstrated, including three-dimensional optical data storage and optical limiting and switching.

Introduction

Recently, nanocomposite materials with periodic structures have stimulated great interest in Materials Science because of their potential applications as chemical sensors, optical data storage devices, and optical limiters and switches.[1] In the "bottom-to-top" approach to fabrication of such materials functionalized particles with a very narrow size distribution and dimensions varying from several hundred nanometers to several microns can be viewed as the building blocks or structural units. Furthermore, the utilization of submicrometer particles with a core-shell or multilayer morphology allows one to obtain complex compositional and structural patterns in the ultimate nanocomposite material.

Our group developed a "core-shell" strategy for fabrication of periodically nanostructured polymer-based materials.[2] An overview of the core-shell approach is given in Figure 1. The essential feature of the core-shell particles synthesized in Stage A is a specific relation between the glass transition temperatures, T_g, of the core-forming polymer (CFP) and the shell-forming polymer (SFP): the glass transition temperature of the SFP should be substantially lower than that of the CFP, that is, $T_{g,SFP} < T_{g,CFP}$. The core-shell microspheres are assembles in a periodic array in Stage B and annealed at the temperature $T_{g,SFP} < T_{annealing} < T_{g,CFP}$ (Stage C), at which the SFP softens and flows, forms ultimately a continuous matrix,

 CCC 1022-1360/00/$ 17,50+.50/0

while the CFP remains intact and produces the disperse phase of the nanocomposite material. This strategy provides several levels of control over the structure and function of the nanostructured material, that is, over particle dimensions, number density, and the composition of the particles and the matrix. First, core-shell particles can contain organic or inorganic polymers in the core and/or in the shell. Second, a combination of inorganic cores and polymer shells can be used. Finally, core- and shell-forming polymers can be physically doped or chemically functionalized with different species tailoring interesting novel properties to the ultimate material. In particular, when the core and the shell have different optical properties, e.g., refractive index, nonlinearity, or fluorescence, the ultimate periodically structured material can perform as a photonic crystal.

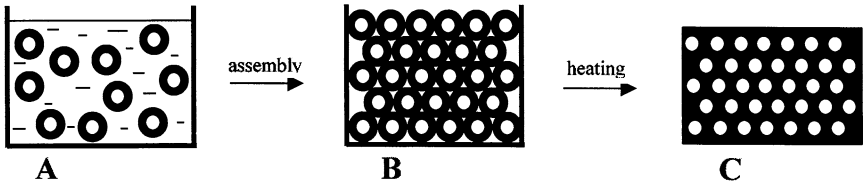

Figure 1: Schematics of the "core-shell" approach to producing polymer-based nanostructured materials. A: synthesis of core-shell particles; B: assembly of core-shell particles in periodic arrays; C: heat processing of core-shell particles to produce nanocomposite material.

Three different methods used in the preparation of core-shell particles are shown in Fig. 2. Interfacial polymerization of the shell on the surface of a polymeric or an inorganic core (Fig. 2a) is preferred when the core-forming material (CFM) and the shell-forming polymer (SFP) have a reasonably high compatibility. When the CFM and the SFP have a high interfacial tension, electrostatic interaction approach is the method of choice.[3] In this approach, dispersions of oppositely charged large particles of the CFM and small particles of the SFP are mixed and annealed, as shown in Fig. 2b. Upon mixing, electrostatic attraction between the beads leads to the formation of individual monodisperse heterocoagulates. Annealing them at the temperature exceeding T_g of the SFP results in the formation of core-shell particles.

Finally, organic or inorganic cores can be encapsulated with a polymeric shell by controlled phase separation technique, as shown in Fig. 2c.[4] In this approach, particles of the CFM are dispersed in the solution of the SFP. Controlled phase separation of the SFP solution is induced by either changing temperature or adding a non-solvent. Precipitation of the SFP on the core surface, accompanied by heat processing results in the formation of core-shell

particles.

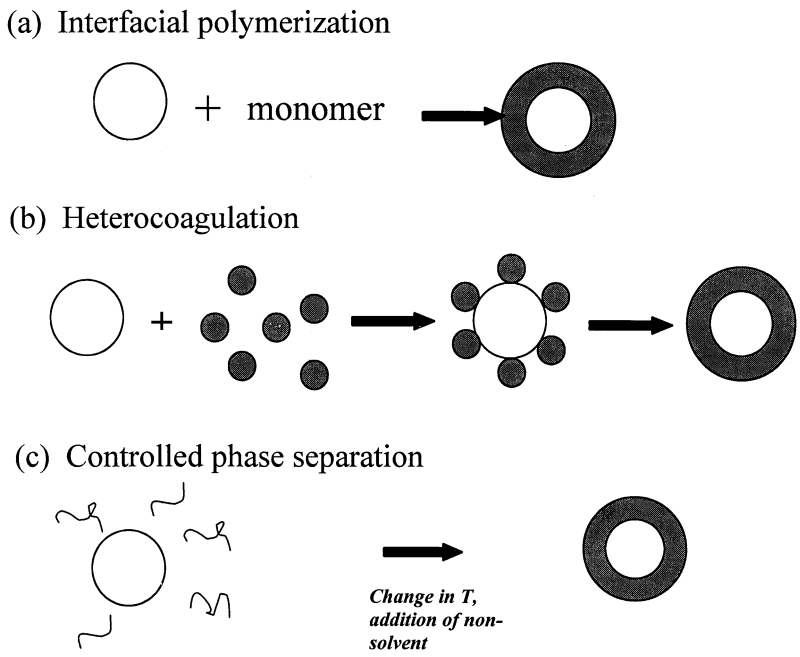

Figure 2: Methods used for preparation of core-shell particles.

In this paper we focus on interfacial polymerization and controlled heterocoagulation which have been extensively utilizing in our laboratory to produce core-shell particles. In addition, we also demonstrate and discuss several potential applications of these particles in fabrication of polymer materials with advanced optical properties.

Polymeric Core-Shell Particles Obtained by Interfacial Polymerization

Emulsion polymerization is a common technique used in production of organic core-shell particles. Extensive studies have been carried out to examine the effect of polymer/water and polymer/polymer interfacial tension,[5-7] the effect of initiator,[8,9] the mode of monomer addition (batch *vs.* semi-batch),[10-12] and the effect of cross-linking agents[13] on morphology of the composite latex particles.

Here, we modified the approach introduced by Rudin *et al.*[14] to prepare monodisperse core-shell particles with the size varying from ca. 200 nm to 1.5 μm. Core-shell particles with a

hard core and a softer shell were synthesized to produce optically responsive polymer nanocomposite material with a periodic structure shown in Fig. 1c.[15] The core forming polymer, CFP, was a homopolymer of poly(methyl methacrylate), PMMA, and the SFP was a random copolymer of poly(methyl methacrylate) and poly(butyl methacrylate), P(MMA-co-BMA).[16] The CFP was functionalized with a small amount of 2-[methyl-(7-nitro-2,1,3-benzooxadiazol-4-ylamino]ethyl-2-methyl methyl methacrylate (NBD-MMA), a fluorescent dye-labelled comonomer. Ethylene glycol dimethacrylate (EGDMA) was used as a cross-linking agent to suppress diffusion of dye-labelled molecules from the core to the shell.

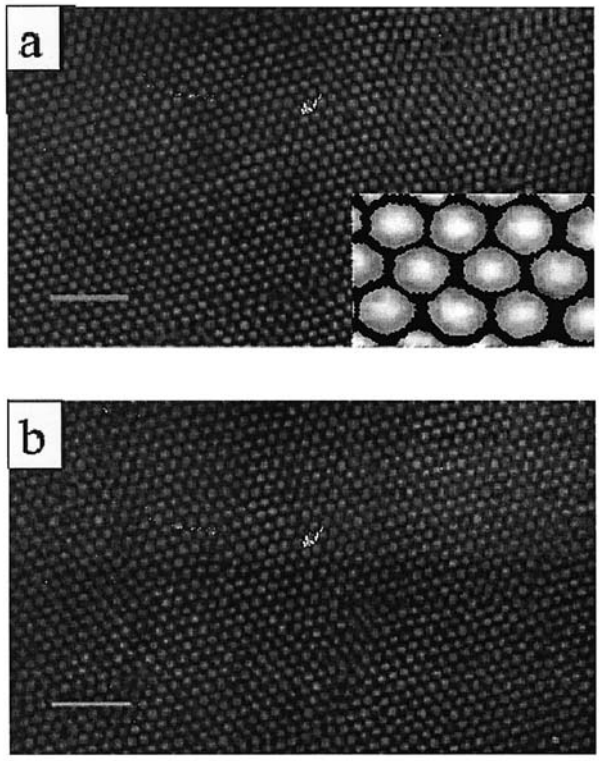

Figure 3. Laser confocal fluorescent microscopy (LCFM) image of the nanostructured material prepared from core-shell particles with rigid 650 nm PMMA cores and 205 nm P(MMA-co-BMA) shells. (a) surface; (b) 30 μm below the surface. Scale bar is 10 μm.

It was found that in order to produce a void-free material, the minimum thickness of the shell had to be at least $0.2r_c$, where r_c is the core radius. The glass transition temperature of the

P(MMA-co-BMA) shell was tuned to 90 °C by adjusting the MMA/BMA ratio to 2/1, while the glass transition temperature of the core was 134 °C. A continuous nanocomposite film was formed by slowly settling dispersion of core-shell particles at room temperature and then annealing the array at 110 °C, that is, about 20 °C above $T_{g,CFP}$. Figure 3 shows the surface and bulk morphologies of the nanocomposite, examined by laser confocal fluorescence microscopy (LCFM). The core has a diameter of 640 nm and the shell has a thickness of 205 nm. As shown in the images, the SFP forms a continuous optically inert phase (dark background), whereas fluorescent CFP particles remain intact (bright domains). The distance between the fluorescent cores is controlled by the thickness of the shell.

The core-shell approach to fabrication of periodically nanostructured materials was further modified by using three-layer latex particles with fluid cores.[17] Latex particles with a fluid core, rigid shell 1, and matrix-forming shell 2 were used as the building blocks in the fabrication of polymer nanostructured materials with liquid inclusions.[18] This work was motivated by the fact that the speed of photochemical reactions of dyes and chromophores could be significantly increased at temperatures exceeding the T_g of the host polymer.[19] In our work, fluid core particles having T_g = –1.6 °C and an average diameter of 300 nm were synthesized by copolymerizing butyl acrylate (BA), and MMA in the weight ratio of 1.5. The CFP were copolymerized with a small amount of NBD-MA and cross-linked with 1.5 mol % of EGDMA. In the second stage, the fluid cores were encapsulated with a thin rigid shell by copolymerizing BA and MMA in the BA/MMA weight ratio of 0.05. The challenge in synthesis of these fluid core-hard shell particles was to suppress rupture of shell 1, which released the fluorescent CFP in the surroundings. The rupture phenomenon occurred during the synthesis of the rigid shell stage at 80 °C and/or during cooling of the core-shell particles from 80 °C to room temperature. This feature was caused by the difference in thermoexpansion coefficients of the CFP and SFP-1, which generated pressure gradients in shell 1. It was found that rapture was closely related to the extent of cross-linking of the SFP-1. An increase in the amount of EGDMA to 9 mol % resulted in an increase of Young modulus of the SFP-1 sufficient enough to suppress shell rupture. The second shell (SFP-2) was consequently synthesized on the surface of the bilayer particles by copolymerizing MMA and BMA in the weight ratio of 1/1. The specific relationship between the glass transition temperatures, T_g's, of the polymers incorporated into the core-shell particles was $T_{g,CFP} < T_{g,,SFP-2} < T_{g,SFP-1}$. Nanocomposite polymeric films were obtained by heat processing of the arrays of three-layer particles at temperature, $T_{gSFP-2} < T_{ann} < T_{g,SFP-1}$. The morphology of the

nanostructured material was studied by examining the distribution of the fluorescent dye in the polymer film.

Figure 4a shows LCFM image of the nanocomposite material obtained from the three-layer particles with fluid cores, while Fig. 4b illustrates the morphology of the control sample, prepared from the dispersion of the two-layer core-shell particles with rigid fluorescent cores. The control sample obtained from the core-shell particles with rigid PMMA cores and P(MMA-co-BMA) shells showed a higher optical contrast between the particles and the matrix, as shown in Fig. 4b. However, the film obtained from the three-layer particles with 9 mol % EGDMA in SFP-1 also had a reasonably high contrast, indicating that rupture of the SFP-1 was essentially suppressed.

In the next step, the distribution of the fluorescence species between the CFP, SFP-1, and SFP-2 was examined quantitatively. All LCFM images were taken at the same magnification at depth 10 μm below the surface of the sample using the same microscope settings (brightness, contrast, intensity of sample irradiation and the number of scans). The spatial variations of fluorescence intensity in the film prepared from the particles with fluid cores and in the control sample are shown in Fig. 4c and d, respectively. In fluorescence line profiles, the distribution of the fluorescent dye between the different phases in the films was characterized by the peak-to-well height, the width of the peaks, and the average brightness of the fluorescent domains. A contrast parameter, CP, calculated as the average of 50 values of the peak-to-well heights was equivalent to the signal-to-noise ratio in the nanocomposite film, and it characterized the distribution of the fluorescent molecules in the material. The values of the CP were 152 and 135 arb.u. for the films obtained from the control latex and from the three-layer particles, respectively. Thus, the CP value for the film of interest was ca. 89% of the CP of the control film. The average peak widths measured at their half-height were 0.42 and 0.52 μm for the control film and for the films prepared from three-layer particles, respectively. Comparison of these values with the diameter of the core particles of 0.3 μm showed a somewhat larger size (23 % larger) of the fluorescent domains in the films with liquid inclusions than that in the control film. Finally, the average brightness of the nanostructured films was found by measuring the average fluorescent intensity of the material. The fluorescent intensities of 500 experimental points on the fluorescence line profiles in Fig. 4c were summed up, and the total intensity was divided by the number of points. Since the rigid cores of the control microspheres and the fluid cores of the three-layer microbeads contained the same amount of fluorescent NBD molecules, it was anticipated that the total

fluorescence intensity from the individual polymeric films would be very close, irrespective of the distribution of dye molecules in the nanocomposite material. Indeed, the values of average brightness for the control sample and for the polymeric films obtained from the three-layer microbeads were 151 and 141 arb.u., respectively.

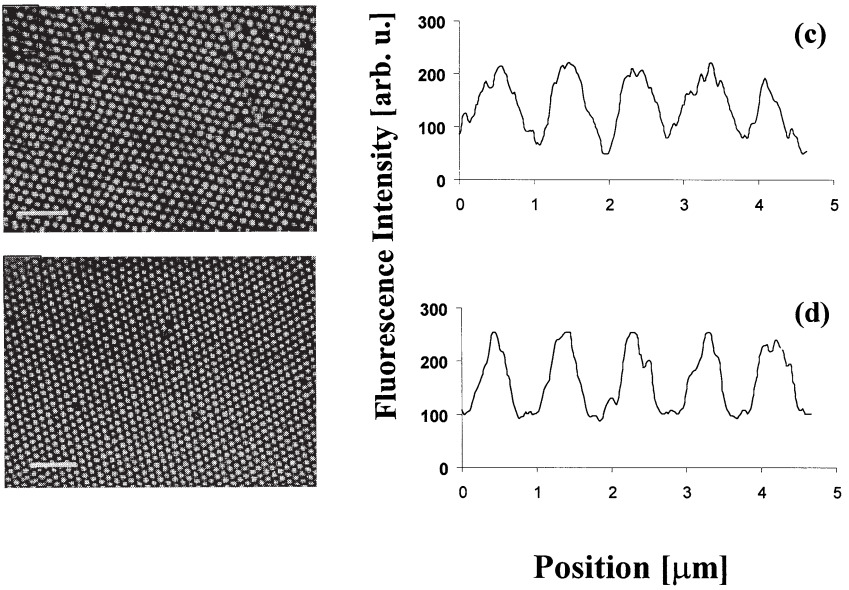

Figure 4. LCFM images of the nanostructured material obtained from particles with fluid cores (a) and core-shell particles with rigid cores (b). The images are taken 10 μm below the surface. Scale bar is 10 μm. Fluorescence line profiles: (c) films obtained from three-layer particles; (d) film obtained from control sample.

Thus the use of three-layer core-shell particles as the building blocks led to the formation of the periodically nanostructured material with liquid inclusions, in which the spatial variation in fluorescent properties was close to that in the control film built from the core-shell particles with rigid cores. The three-layer morphology of the particles, in particular, the existence of the intermediate highly cross-linked shell 1 was extremely important in the fabrication of such materials, since SFP-1 formed a rigid wall confining fluid "containers" and suppressing the release of the fluid fluorescent CFP into the surroundings.

Furthermore, it was found that in the core-shell approach covalent attachment of dyes or chromophores to the CFP or SFP accompanied by cross-linking of the corresponding polymer was vital for the preparation of the nanostructured material with a strong modulation in optical

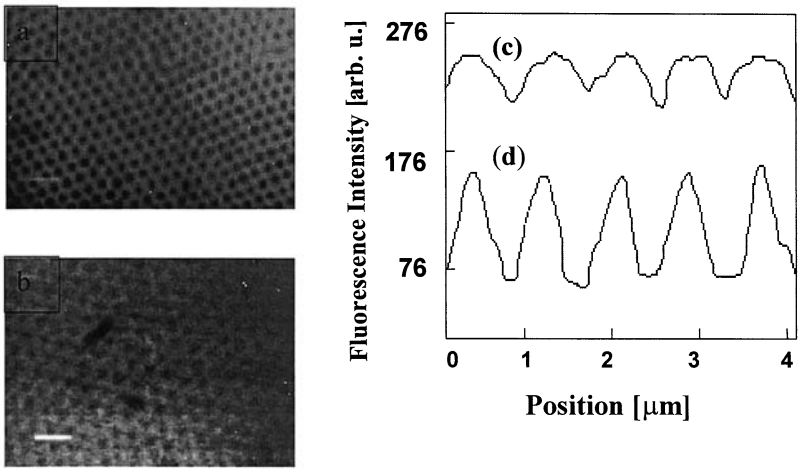

Figure 5: LCFM images of the nanostructured material obtained from core-shell particles with fluorescent matrix. (a) NBD dye is covalently attached to the crosslinked SFP; (b) NBD dye is mixed with the SFP. The scale bar is 2 μm. Fluorescence line profiles in (c) and (d) correspond to samples (b) and (a), respectively.

properties.[20] The effect of chemical attachment of dyes and polymer cross-linking versus physical incorporation of dyes in a polymer was demonstrated for materials with "inverse" structure. Figures 5a and b show the morphology of such materials obtained from the core-shell particles with fluorescent shells. When NBD-MA was copolymerized with P(MMA-co-BMA) shell-forming polymer and the SFP was cross-linked with EGDMA, high optical contrast between the fluorescent matrix and the particles was obtained, as shown in Fig. 5a. Blending of the dye with the same SFP (Fig. 5b) led to a substantial reduction in optical contrast, as a result of the dye-labeled molecules diffuse between the cores and the shells during synthesis and /or annealing. These results were further confirmed by analysis of the fluorescence line profiles as described above. Figure 5c shows the fluorescence line profiles obtained from image analysis of Fig. 5a and b. In the films obtained from the latex particles in which the dye molecules were covalently attached to the crosslinked SFP (bottom curve), the average value of CP was ca. 2.5 times higher than that obtained from the particles in which the dye molecules were physically mixed with the SFP (top curve). Covalent attachment of the NBD dyes to the non-crosslinked SFP led to the intermediate mean value of CP. To conclude, chemical attachment of dye molecules to the corresponding cross-linked

polymer was critical in producing high quality nanostructured materials.

Polymeric and Hybrid Core-Shell Particles Obtained by Controlled Heterocoagulation

Heterocoagulation of large and small oppositely charged colloid particles, accompanied by spreading of small beads over the surface of large spheres (Fig. 2b) offers a promising alternative to synthesis of core-shell particles. This approach is particularly useful for the production of core-shell particles with polar cores and nonpolar shells since preparation of these particles using interfacial polymerization often results in nucleation and growth of secondary particles and/or in synthesis of particles with an "inverse" structure. In the first series of experiments, rigid cores were synthesized from polypyrrole (PPy),[21] a polar polymer with high surface energy, whereas in the second series, inorganic SiO_2-$TiOSO_4$ (SiO_2-TS) cores were used. Both types of particles carried a positive charge.

The choice of PPy as a core-forming polymer was motivated by the fact that core-shell particles with conductive cores and dielectric shells can be used as the building blocks in fabrication of nanostructured materials with periodically modulated conductive properties. In such materials an ordered array of monodispersed spheres synthesized from a conjugated polymer is dispersed in an insulating or a semi-conductive polymer matrix. Nanostructured materials produced in this fashion have potential applications in sensor and nanocapacitor devices, and in nano-resettable fuses. Inorganic SiO_2-TS particles were used to achieve a high refractive index modulation in the ultimate nanocomposite material.

The individual core particles (PPy or SiO_2-TS particles) were mixed with small negatively charged beads of PMMA, P(MMA-co-BMA), or PBMA. Heterocoagulation induced by electrostatic interaction, followed by heating the dispersion at temperature above the glass transition temperature of the polyacrylic particles generated core-shell particles.

PPy core particles were prepared by dispersion polymerization. Interfacial polymerization of PMMA on the surface of PPy using $K_2S_2O_8$, 2,2'-azobis(2-methyl propionitrile) and 4,4'-azobis(4-cyanovaleric acid) as the initiators proved to be problematic. In the first two cases polymer conversion was relatively low (<40%), whereas with the latter initiator, broad particle size distribution was often obtained. In contrast to interfacial polymerization, electrostactically-driven heterocoagulation proved to be an efficient way to the preparation of PPy core-polyacrylate shell particles. To obtain monodisperse core-shell particles with smooth polyacrylic shells several requirements had to be fulfilled. First, monodisperse heterocoagulate

units could be obtained only at the optimum total concentration of particles in the dispersion of ca. 0.1 wt %. In more concentrated systems, notable particle aggregation was observed. Second, a critical number ratio of small-to-big particles, N_S/N_L, existed above which individual monodisperse heterocoagulates were obtained. Figure 6a shows the variation in dimensions of heterocoagulate units as a function of N_S/N_L for 204 nm PPy beads mixed with 48 nm PMMA particles. For N_S/N_L < 84, the mean size of the heterocoagulate units was substantially larger than ca. 300 nm anticipated for individual heterocoagulate units, which

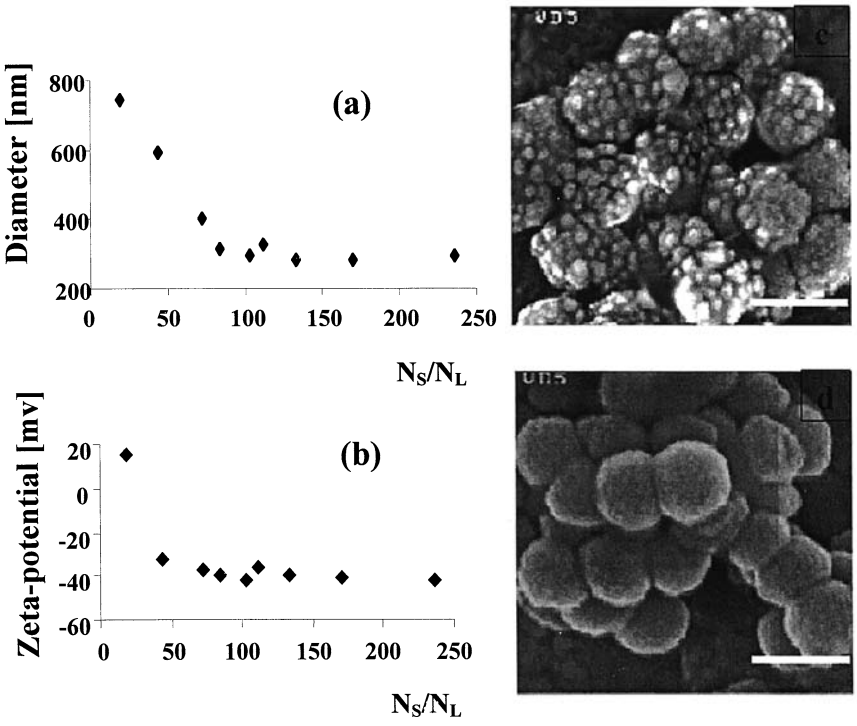

Figure 6. Effect of N_S/N_L on the variation in diameter (a) and electrokinetic potential (b) of heterocoagulate units formed by electrostatically-driven heterocoagulation of 204 nm PPy beads and 48 nm PMMA particles. SEM images of PPy/PMMA-co-PBMA composite particles prior to (c) and after annealing for 23 h annealing at 90 °C (d). Ns/N_L = 180. Scale bar 300 nm.

indicated strong uncontrolled particle aggregation. For 84 < N_S/N_L < 112, the average heterocagulate size gradually reduced to ca. 300 nm and for N_S/N_L > 112, no further change was observed. These results correlated with the variation in ζ-potential of heterocoagulates

(Fig. 6b). In Fig. 6b, the value of ζ-potential gradually decreased and for N_S/N_L= 84 it reached a constant value of – 40 mV, which was close to that of the individual PMMA beads. The dependence of heterocoagulate size and ζ- potential could be explained by bridging of several PPy beads through the small polyacrylic particles, that is, in excess of PPy particles.

The role of charge of cationic and anionic particles was two-fold. A large contrast between the charges of PPy and polyacrylic particles resulted in a strong driving force for heterocoagulation, however repulsion between the similarly charged small beads adsorbed on the core surface counteracted their dense packing. Low packing density of the small particles resulted in a raspberry structure of the shells.[22] Figure 6c and d show PPy/PMMA-co-PBMA heterocoagulate units imaged before and after heat processing. For optimized N_S/N_L after annealing the raspberry structure of the heterocoagulate units was substantially smeared.

A similar approach was used for the preparation of hybrid core-shell particles. SiO_2-TS particles encapsulated with P(MMA-co-BMA) copolymer. Monodisperse SiO_2 particles with dimensions varying from 300 to 800 nm were prepared using sol-gel process. These particles were then coated with TS using a modified approach of Matijevich.[23] The process of coating was driven by electrostatic attraction between the negatively charged silica particles and positively charged TS clusters at pH = 4; therefore TS coating had a raspberry structure.[24]After heterocoagulation, the SiO_2-TS beads carried a small positive charge. Figure 7a shows the results of Energy Dispersion X-Ray analysis of the composite SiO_2-TS microspheres. In this graph the weight ratio TS/SiO_2 in the particles is plotted as a function of ϕ, the ratio of the mass of TS in the system to the total surface area of silica particles. When ϕ increased, the fraction of TS in the composite particles grew due to the more complete coverage of the SiO_2 core. On the basis of the EDS measurements, for the complete coverage of the silica cores with TS achieved at ϕ = 0.085 g/cm^2, the weight ratio TS/SiO_2 reached ca. 35%, this ratio corresponded to ca. 26 wt % of TS in the composite particles.

Encapsulation of the composite SiO_2-TS cores with a polymeric shell was accomplished via electrostatic heterocoagulation of the cationic SiO_2-TS particles and anionic P(MMA-co-BMA) microbeads. The requirements for controlled heterocoagulation were similar to those described for PPy-polyacrylic particles. Upon heating SiO_2-TS/P(MMA-co-BMA) heterocoagulates obtained at sufficiently high N_S/N_L formed core-shell particles with reasonably smooth shells. Figures 7b and c show the SEM images of the SiO_2-TS/P(MMA-co-BMA) heterocoagulates before and after annealing, respectively. A near complete polymer spreading was observed and the surface roughness of the hybrid particles was almost

smoothed over. Some voids remaining in the P(MMA-co-BMA) shells resulted presumably from the polymer flow and penetration in the gaps between the TS clusters adhering to the surface of silica cores.

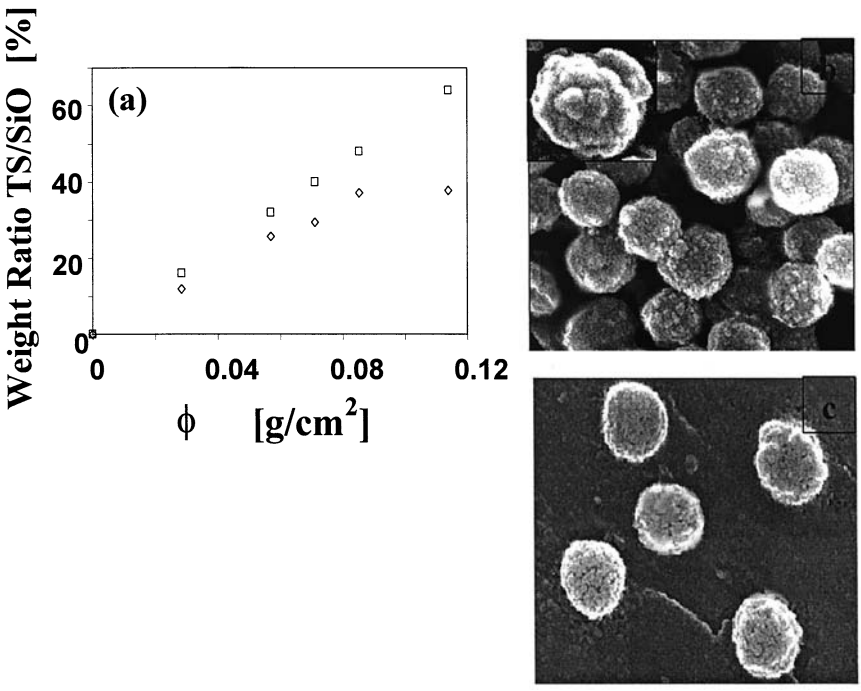

Figure 7. (a) Experimental (◊) and calculated (□) weight ratios of TS/SiO_2 in th composite particles plotted as a function of the weight ratio of TS/surface area of silica. (b) SEM images of SiO_2-TS/PMMA-PBMA hybrid particles obtained at N_S/N_L = 119 (c) after heat processing.

Optical Applications of Polymer-Based Materials Produced from Core-Shell Particles

Three-dimensional optical data storage. Further progress in information technologies depends critically on the development of new materials for high-density optical memory storage. As an alternative to two-dimensional (2D) data storage, 3D media promise a dramatic increase in memory capacity since the storage density scales as $1/\lambda^2$ and $1/\lambda^3$, where λ is the wavelength of the reading beam, for 2D and 3D optical memories, respectively. Nanostructured materials with a periodic modulation in optical properties (photonic crystals) show great promise as a medium for high-density 3D optical data storage.[25]

Polymer nanocomposite material with a periodic close-packed array of fluorescent particles periodically embedded in an optically inert matrix (Fig. 3) was examined with respect to 3D optical writing/reading. In the two-photon recording experiments, we employed a Biomedical Photometrics confocal microscope equipped with a home-built femtosecond laser. Optical recording in the polymer nanocomposite was achieved by addressing and photobleaching the individual fluorescent particles. Pulses were typically 100 fs centered at 844 nm. Reading out of the resulting bit pattern was accomplished with the same two-photon confocal microscope using 0.5 mW average power laser fluences. Figure 8a shows a two-dimensional plane of the nanostructured material located at the depth of ca. 200 mm, in which optical recording was carried out by photobleaching fluorescent particles for approximately 150 ms at 5 mW of average power. A photobleached fluorescent bead appears as a black spot in the periodic structure of the nanocomposite. Since the absorption peak of the dye is 476 nm and the polymer is transparent in the visible and near IR range, absorptive coupling of the laser light occurred through two-photon absorption by the NBD dye. The photobleaching of the NBD

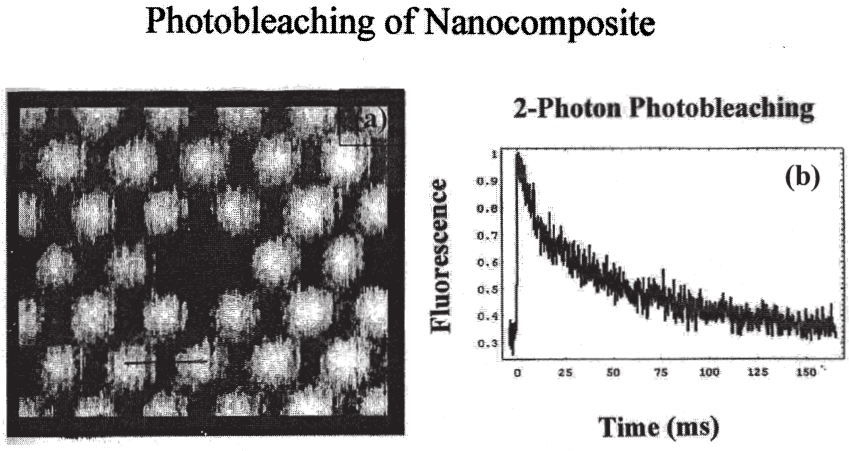

Figure 8: Two-photon writing in a 3D nanostructured material induced by local photobleaching of the fluorescent dye incorporated into the core particles. (a) Structure of the addressed plane located 200 μm from the top surface. The center-to-center particle distance is 1 μm. (b) Fluorescence decay *vs*. time for the addressed particle.

dye caused by photooxidation was irreversible, providing the basis for permanent data storage.

As can be seen from Fig. 8b showing a decay of fluorescence in time, a contrast ratio of 2:1 in fluorescence intensity of unbleached to bleached particles, respectively, was achieved after an exposure time of 20 ms (Fig. 8b).

In these experiments, core-shell particles with rigid fluorescent cores were used as the building blocks of the nanostructured recording media. Preliminary results obtained in our laboratory showed that NBD dye was photobleached substantially faster when the nanostructured material was fabricated from the three-layer particles with a fluid fluorescent core.

Optical limiters and switches. Recently, Sargent *et al*[26] have demonstrated that nanostructured materials with periodically modulated nonlinear refractive index have potential applications in optical limiting and switching devices. In such materials, the linear refractive index of the particles and the matrix are very close, whereas their nonlinear refractive indices are different and opposite in sign. This feature can be accomplished by incorporating nonlinear optics species in the core and in the shell of the core-shell particles used as the structural units in the fabrication of such materials. Covalent attachment of organic species, e.g., azobenzenes to the CFP or SFP or doping of the CFP or SFP with inorganic nanocrystals (quantum dots) proved to be a very efficient method in tuning optical limiting properties of nanocomposite films. Currently, these experiments are conducted in our laboratory in collaboration with Sargent's group.

Conclusion

The core-shell strategy shows a broad avenue to the fabrication of advanced polymer materials. A large number of possible combinations of the core-forming materials and the shell-forming polymers allows for production of nanostructured materials with various structural and compositional patterns. A particular method used for the preparation of core-shell particles depends on the corresponding polymers and should be chosen with caution. Core-shell particles with tunable optical properties great potential applications as high density three-dimensional optical data storage and optical limiting.

[1] Lee, K., Asher, S.A. *J. Am. Chem. Soc.* **2000**, *122*, 9534; Siwick, B.J., Kalinina, O. Kumacheva, E., Miller, R.J.D., Noolandi, J. *J. Appl. Phys.* **2001**, *90*, 5328; Brzozowski, L., Sargent, E.H. *IEEE J. Quant. Eletron.* **2000**, *36*, 550.

[2] Kumacheva E., Kalinina O., Lilge L. *Adv. Mater.* **1999**, *11*, 231.

[3] Okubo M., Lu Y. *Col. Surf.* **1996**, *109*, 49; Ottewell R.H. Schofield A.B., Waters J.A., Williams N.S. *J. Col.*

Polymer Sci. **1997**, *275*, 274; Furusawa K., Velev O.D. *Col. Surf. A* **1999**, *159*, 359.
[4] Dudnik V., Sukhorukov G.B., Radtchenko I.L., Mohwald H. *Macromolecules* **2001**, *34*, 2329.
[5] Daniel J.C. *Makromol. Chem. Suppl.* **1985**, 10/11, 359.
[6] Sutterlin N. *Makromol. Chem. Suppl.* **1985**, 10/11, 403.
[7] Min T.I., Klein A., El-Aasser M.S., Wanderhoff J.W. *J. Polym. Sci., Polym. Chem.* **1983**, *21*, 2845.
[8] Chen Y-C., Dimonie V.L., El-Aasser M.S. *J. Polym. Sci., Polym. Chem.* **1991**, *42*, 1049.
[9] Jonsson J-E., Hassander H., Hansson L.H., Tornel B. *Macromolecules* **1994**, *27*, 1932.
[10] Okubo M., Yamada Y., Matumoto T. *J. Polym. Sci., Polym. Chem.* **1980**, *18*, 3219.
[11] Lovell P.A., McDonald J., Saunders D.E.J., Young R.J. *Polymer* **1993**, *34*, 61.
[12] Jonsson J-E., Hassander H., Hansson L.H., Tornel B. *Macromolecules* **1991**, *24*, 126.
[13] Hu R., Dimonie V.D., El-Aasser M.S. *J. Appl. Polym. Sci.* **1995**, *58*, 375.
[14] O'Callagham K.Y., Paine A.Y., Rudin A. *J. Appl. Polym. Sci.* **1995**, *58*, 2047; O'Callagham K.Y., Paine A.Y., Rudin A. *J. Appl. Polym. Sci.* **1995**, *33*, 1849.
[15] Kalinina O., Kumacheva E. *Macromolecules* **1999**, *32*, 4122.
[16] Kalinina O., Kumacheva E. *Macromolecules* **2001**, *34*, 6380.
[17] Kalinina O., Kumacheva E. *Macromolecules* **2002**, *35*, 3675.
[18] It was found that core-shell particles with low T_g cores could not be used in the fabrication of nanocomposite material with liquid inclusions due to the release of the fluorescent CFP into the matrix.
[19] Talhavini M., Atvars T.D.Z. *Photochem. Photobiol.A: Chem.* **1998**, 50, 65.
[20] Kalinina O., Kumacheva. E. *Chem. Mater.* **2001**, *13*, 35.
[21] Li H., MSc. thesis, University of Toronto, 2002.
[22] Strictly speaking, a critical packing density required for smooth shell formation could be predicted on the basis of values of interfacial tension between the CFP and the SFP and the size of small particles. For a particular system the distance between the small particles on the surface of large core could be controlled by varying ionic strength of the dispersion medium.
[23] Matijevic E., Hsu W.P., Yu R. *J. Colloid Interface Sci.* **1993**, *156*, 56.
[24] Han J., Kumacheva E. *Langmuir* **2001**, *17*, 7912.
[25] Koroteev N. I., Magnitskii S.A., Tarasishin A.V., Zheltikov A.M. *Laser Physics* **1999**, *9(6)*, 1253.
[26] Pelinovsky D., Sears J., Brzozowski L., Sargent E.H. *J. Opt. Soc. Amer. B: Opt. Phys.* **2002**, *19*, 43